University of Vermont
ScholarWorks @ UVM

Graduate College Dissertations and Theses
Dissertations and Theses

2017

Thermodynamic vs kinetic control of particle assembly and pattern replication

Lizhen Chen
University of Vermont

Follow this and additional works at: https://scholarworks.uvm.edu/graddis

Part of the Chemistry Commons

THERMODYNAMIC VS KINETIC CONTROL OF PARTICLE ASSEMBLY AND
PATTERN REPLICATION

A Thesis Presented

by

Lizhen Chen

to

The Faculty of the Graduate College

of

The University of Vermont

In Partial Fulfillment of the Requirements
for the Degree of Master of Science
Specializing in Chemistry

May, 2017

Defense Date: December 19, 2016
Thesis Examination Committee:

Severin Schneebeli, Ph.D., Advisor
Patrick Lee, Ph.D., Chairperson
Jianing Li, Ph.D.
Adam C. Whalley, Ph.D.
Cynthia J. Forehand, Ph.D., Dean of the Graduate College

ABSTRACT

This research aims to investigate how particles assemble together through thermodynamic and kinetic control. Particle assembly with thermodynamic control is achieved in part due to electrostatic attraction between particles. Electrostatic attraction between particles can be achieved by functionalizing polystyrene or SiO_2 particles with different charges. Particles with different charges will come together in solution slowly and self-assemble to form ordered crystals with different patterns based on size and charge ratios of two oppositely charged particles. Kinetic control of particle assembly is achieved by pattern aided exponential amplification of nanoscale structures. Some of these nanoscale structures are difficult to build with other conventional synthetic methods. On the other hand, as for kinetically controlled particle replication, the patterns can be synthesized by one of two ways i) crystal products which are produced by thermodynamically controlled particle assembly or ii) single particle deposition. Specifically, kinetically controlled particle assembly focuses on constructing SiO_2 particles. Exponential replication of SiO_2 particles is achieved by growing a "bridge layer", between templates of SiO_2 particles and next generation SiO_2 replicas. By dissolving the bridge layer, two times the amount of the SiO_2 particles with the shape of the original templates can be formed. In the next generation, all the particles serve as template particles. Thus, after n cycles of replication, 2^n amount of products can be formed. If successful, particle assembly can be thermodynamic controlled and particle exponential replication can be kinetical controlled, which will enable new ways to build particles with well-defined shapes from readily available building blocks.

Key words: Thermodynamic and kinetic control, Particle assembly, Exponential replication, SiO_2, Well-defined shape, Pattern growth

ACKNOWLEDGEMENTS

TABLE OF CONTENTS

Page

LIST OF TABLES

LIST OF FIGURES

CHAPTER 1: Thermodynamically Controlled Particle Self-assembly

1.1. Introduction

This project focuses on using thermodynamics to control particle self-assembly to explore how ordered structures at the macro-meter scale can be created efficiently with bottom-up strategies. Small building blocks such as colloids and nanoparticles are used in bottom-up assembly to obtain desired target structures (Fig 1b). On the other hand, top-down methods use precise macroscopic methods, such as lithography with photons, electrons, and atoms to break down larger starting materials into desired target structures (Fig 1a), which are technically less assessable, because more complicated instruments are required, compared to bottom-up assembly methods. In this project, bottom-up assembly methods are used to make programmable colloidal crystals. [2,3]
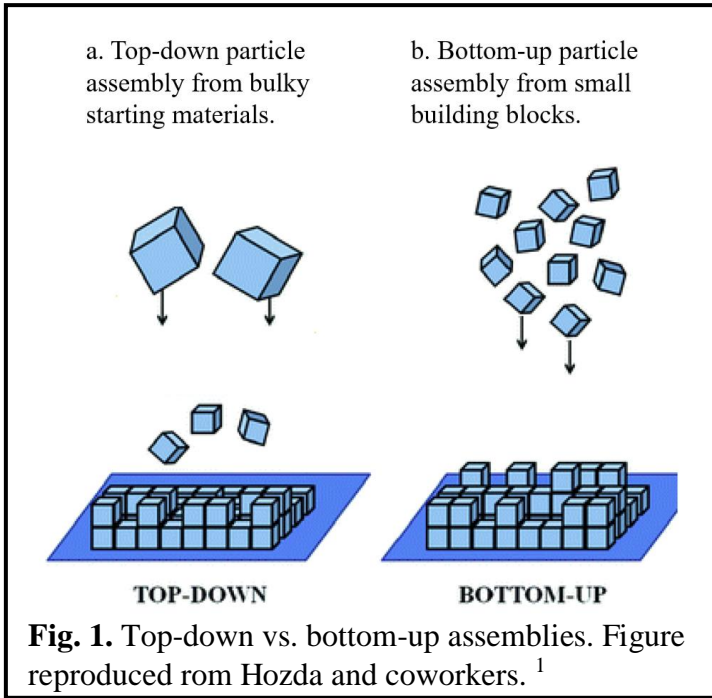
In order to understand how particles can be bottom-up assembled, it is necessary to explain thermodynamic control. Thermodynamically controlled self-assembly is used to describe particles coming together to form ordered structures in a relatively long time scale in order to get the lowest free energy of the

a. Top-down particle assembly from bulky starting materials.

b. Bottom-up particle assembly from small building blocks.

TOP-DOWN

BOTTOM-UP

Fig. 1. Top-down vs. bottom-up assemblies. Figure reproduced rom Hozda and coworkers. [1]

1

structures.[4] The driving forces of self-assembly could be external, for instance electric or magnetic fields, or could be internal, for instance intermolecular hydrogen bonding and Van der Waals forces. Control of the shape, size, and attached functional groups has been reported to help particle self-assembly.[5] The interaction strength between particles can be manipulated by modifying particles with different function groups and the intensity of attached functional groups.[6] In this project, Van der Waals forces, and electrostatic attraction are used to aid particles with different charges coming together to form larger structures or a colloid with thermodynamic control.
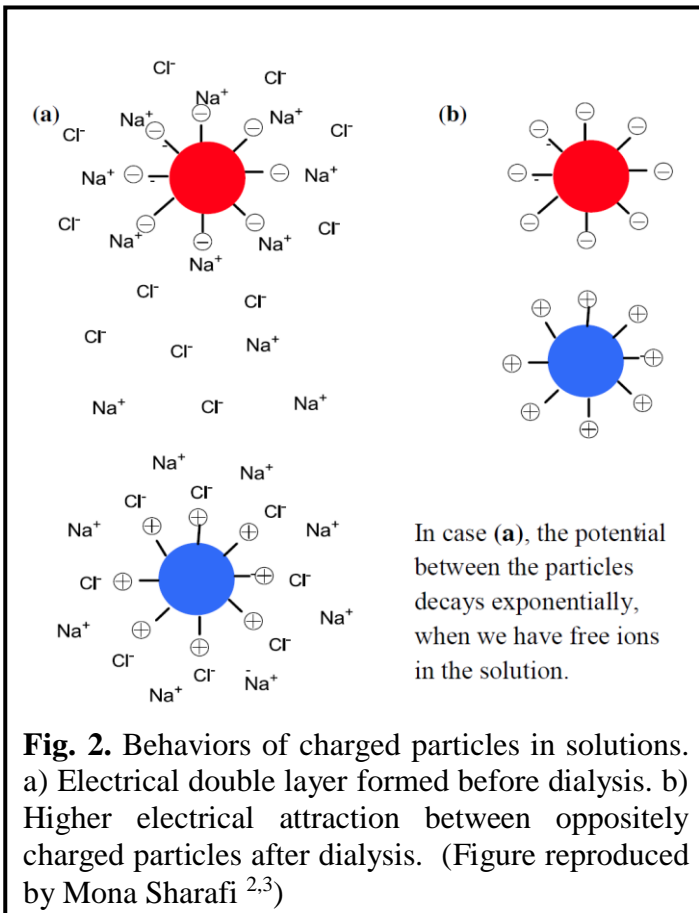
Electrostatic attraction is applied to drive the particle assembly process. When particles are modified by charged functional groups like $-NH_2^+$ and $-SO_3^-$, they become charged.[4,7] The resulting charged surface interacts with dissolved counter-ions in the solution and consequently an electrical double layer surrounding the charged particles forms (Fig 2a).[4] This effect will decrease the effective charges on the particle surfaces, which is not desired. In order to decrease this effect and keep the

In case (a), the potential between the particles decays exponentially, when we have free ions in the solution.

Fig. 2. Behaviors of charged particles in solutions. a) Electrical double layer formed before dialysis. b) Higher electrical attraction between oppositely charged particles after dialysis. (Figure reproduced by Mona Sharafi [2,3])

highest effective charges on particle surfaces, membrane dialysis is used to remove counter ions.   A representation of particles with higher effective charges after dialysis is shown in Fig 2b. Relatively long duration dialysis is the essential step of the thermodynamic control method to bring particles with different charges together to form more ordered, self–assembled shapes. The morphology of self-assembled products depends on the size, shape and charge of the particles. The charges on the particles can be characterized by using methods such as zeta potential Nano seizer, FTIR, Raman, and XPS spectroscopies and can be predicted by computer simulations.   Different assembled structures can be formed when the charge or size of the particles is altered. For example, if oppositely charged
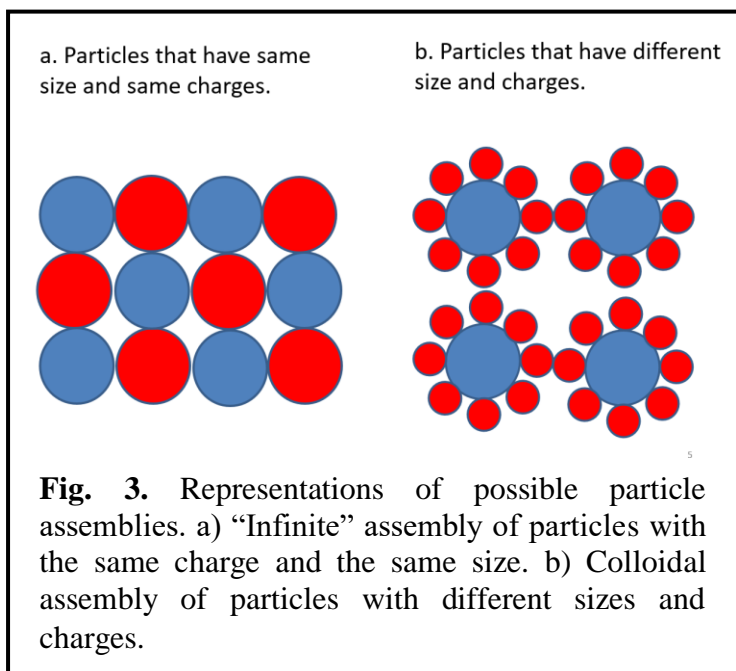
Fig. 3. Representations of possible particle assemblies. a) "Infinite" assembly of particles with the same charge and the same size. b) Colloidal assembly of particles with different sizes and charges.

particles have the same size and are functionalized with same potential, "infinite" crystalline arrays of particles are expected to form. Fig. 3a shows one of the most stable "infinite" assembly structures that can be formed by oppositely charged particles in the same size.[8] On the other hand, when particles with either different sizes or different charges are assembled, smaller or less charged particles are going to surround larger highly charged particles (Fig 3b).

This proposed techniques will likely enables us to make more controlled ionic crystals with different morphologies that can be applied to chemical catalysis, and photonics.[9,10] In order to strengthen particle-particle interactions, which would better facilitate the assembly of controlled particles or colloids, particles or colloids with higher effective charges after dialysis are mixed and allowed to stand in order to reach thermodynamic equilibrium. Membrane dialysis is an efficient tool used to remove the free ions in a solution to generate colloidal counter-ions[11] as well as to thermodynamically control the assembly processes. In order to make it easier to observe the assembly under microscopies, particles with different sizes and shapes are synthesized. These particles can potentially be functionalized with different charges and assembled with thermodynamic control methods to form more ordered structures and crystals.

The self-assembled structures depend on the concentration, size, surface charge and environment of the oppositely charged particles. These structures hold great promise for a variety of applications, ranging all the way from templated polymerization of charged molecules to the assembly of charged nano-objects, catalysis and photonics.[12,13]

1.2. Results and Discussions

Poly (styrene-co-4-vinylbenzyl chloride) (PS-Cl) particles were chosen as the first generation candidate of the thermodynamically control particle assembly. This material was chosen because it can potentially be functionalized with different charged functional

groups on the -Cl ends.   Another advantage of using PS-Cl particles is that they are intrinsically neutral compared to other particles.

Fig. 4. SEM images of PS-Cl particles in different sizes and shapes. a) 4 um Flower-structured PS-Cl particles. b) 2 um spherical PS-Cl particles.
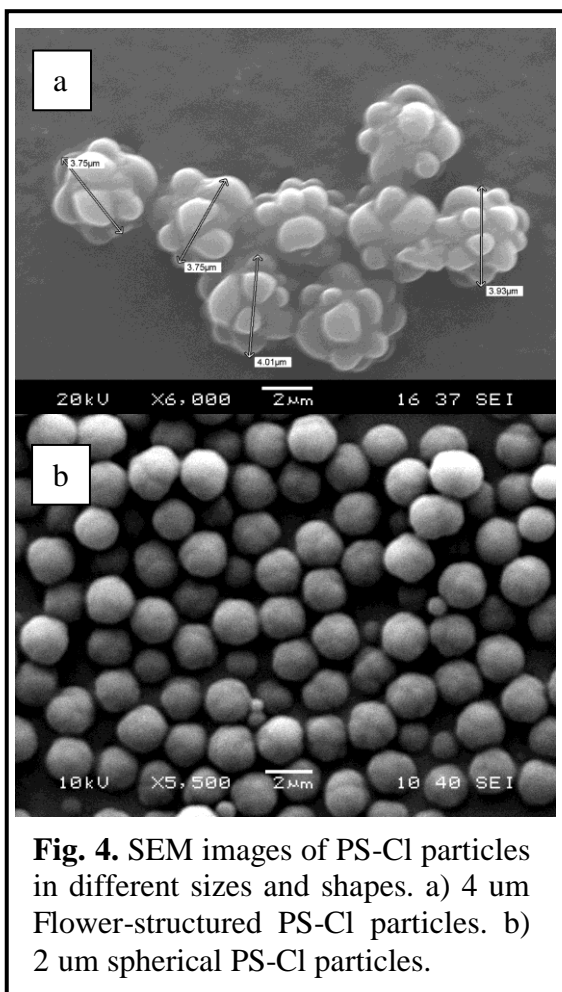
We started our investigation by synthesis of PS-Cl particles in various sizes (400 nm – 10 μm) and shapes using Divinyl-benzene (DVB) as cross-linker to stabilize the particles following previously publish literature done by Asher and coworkers.[14] Uniformed Flower structured PS-Cl particles with diameters around 4 um and spherical PS-Cl particles with diameters around 2 μm were made. Scanning Electronic Microscopy (SEM) images are shown in Fig 4. Spherical PS-Cl particles were sent to Robertson Microlit Laboratories for elementary analysis. The result showed that the particles contained 0.66% Cl element, which confirmed that the copolymer particles with Cl incorporated, which could be functionalized later (Table 1a).

After assuring that Cl was incorporated into the particles, oppositely charged functional groups were added to 2 μm spherical PS-Cl particles by following procedures

5

Table 1. Elementary analysis results from Robertson Microlit Laboratories

	Particle	Element Percentage Result
a	PS-Cl	0.66% Cl
b	PS-Cl (S containing)	0.40% S

Fig. 5. Reaction schemes of functionalization of PS-Cl particles with oppositely charged group.
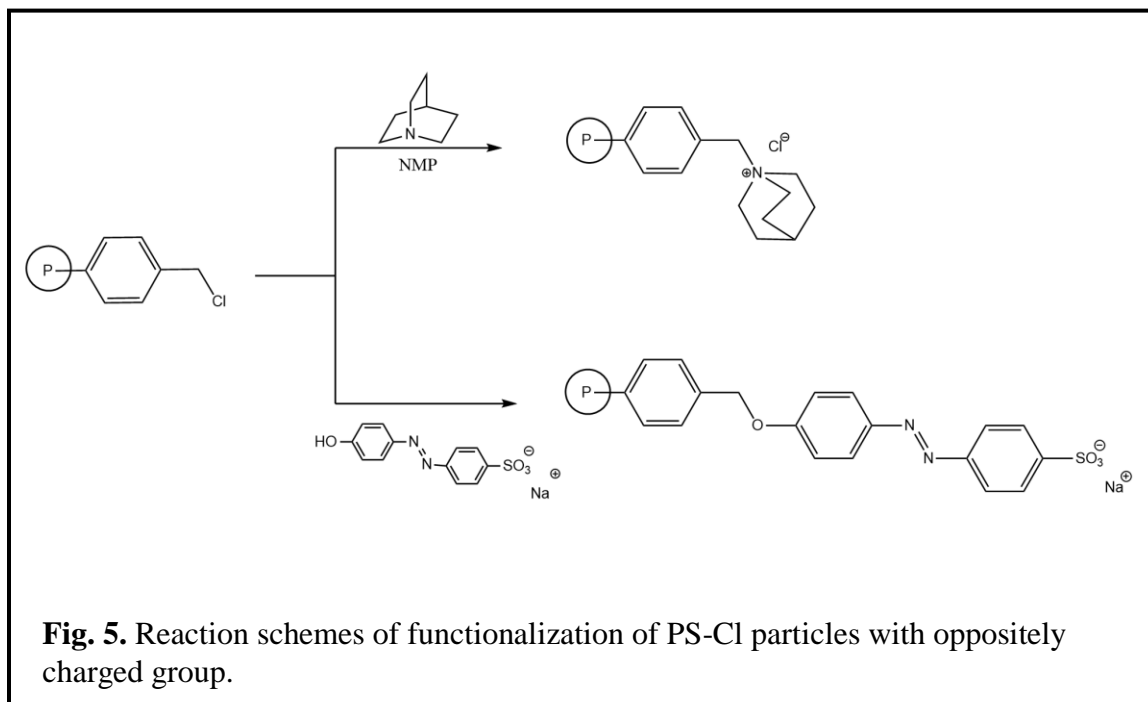
published by Whitesides and coworkers.[15] Reaction schemes are shown in Fig 5. Robertson Microlit Laboratories elementary analysis was carried out again before further assembly. Only the negatively charged particles, which should contain Sulfur if the charged groups were added on successfully, was taken out for the elementary analysis. The result showed that the sample contained 0.4% Sulfur (Table 1b), which meant that the particles were negatively charged. Based on the fact that the similar procedures to add

positively charged on PS-Cl particles were published by Whitesides and coworker in the same paper, we assumed negatively charged groups were successfully added second PS-Cl particle sample. After elementary analysis, charged particle suspensions of both samples were made and two of them were mixed to roughly examine the assembly. When the two suspensions were mixed, no obvious precipitation or aggregation was observed after 24 hours, which is not expected.

Since there was no observable precipitation, we suspect that the particles were not strongly charged, which also can be explained by the result of the two elementary analysis measurements (only trace amounts of Cl and S elements were detected). Therefore, a second generation candidate material, which could be more easily functionalized with more charged groups, was explored.

Fig. 6. SEM images of spherical SiO_2 particles of different sizes. a) 600 nm. b) 200 nm.
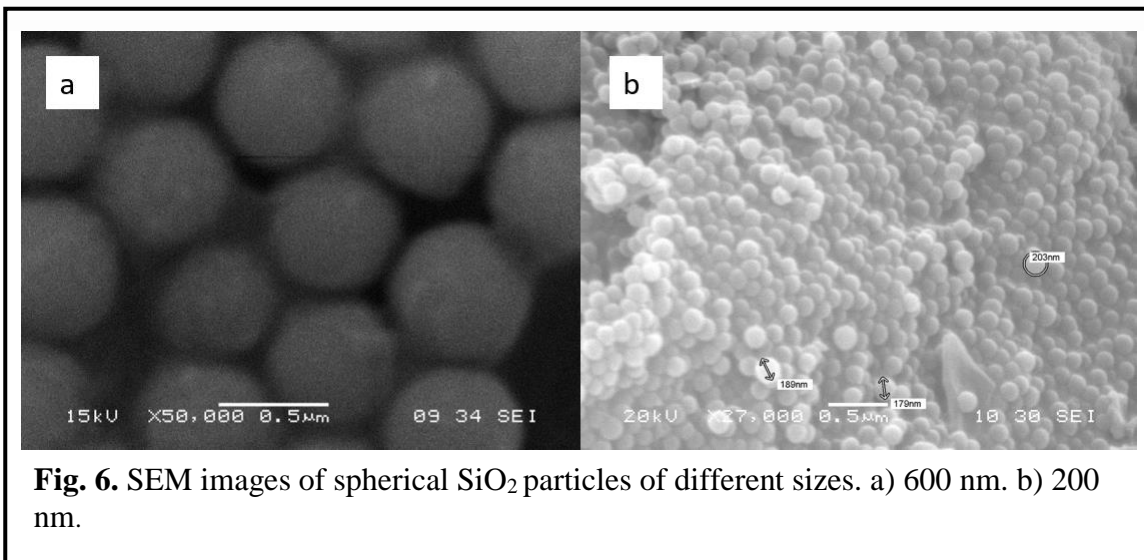
SiO_2 nanoparticles were chosen as the second candidate, because SiO_2 particles can be functionalized easily and are relatively nontoxic and environmental friendly. Uniform spherical 600 nm and 200 nm SiO_2 particles were synthesized with revised

Stöber's process published by Mayer and coworkers[16], and Delville and coworkers[17] (SEM images in Fig 6). Negatively charged $-SO_3^-$ groups were added onto 600 nm SiO_2 particles and positively charged $-N^+(CH_2CH_3)_2$ groups were added onto 200 nm SiO_2 particles following literature procedures.[18] Reaction schemes are shown in Fig 7

Fig. 7. Functionalization of SiO_2 particles with oppositely charged groups.
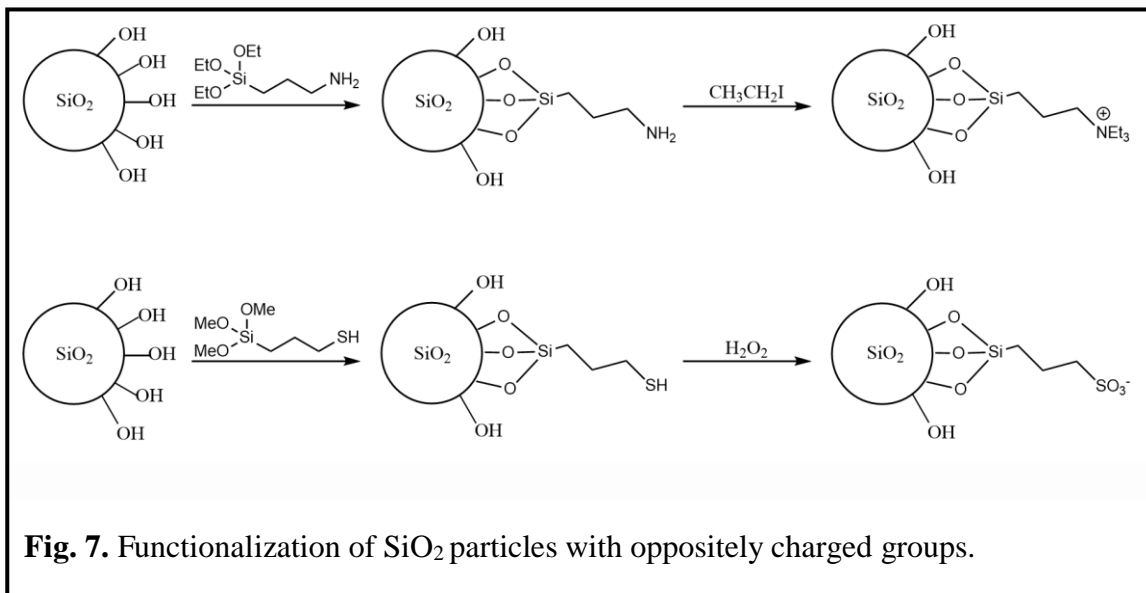
In order make sure that the charged groups were attached to the SiO_2 particles successfully in a sufficient amount, Zeta potentials were measured using a 2SP nano-sizer machine. Approximately 10^9 particles/mL solutions were made for both of the samples. With negatively charged $-SO_3^-$ groups, 600 nm SiO_2 particles showed
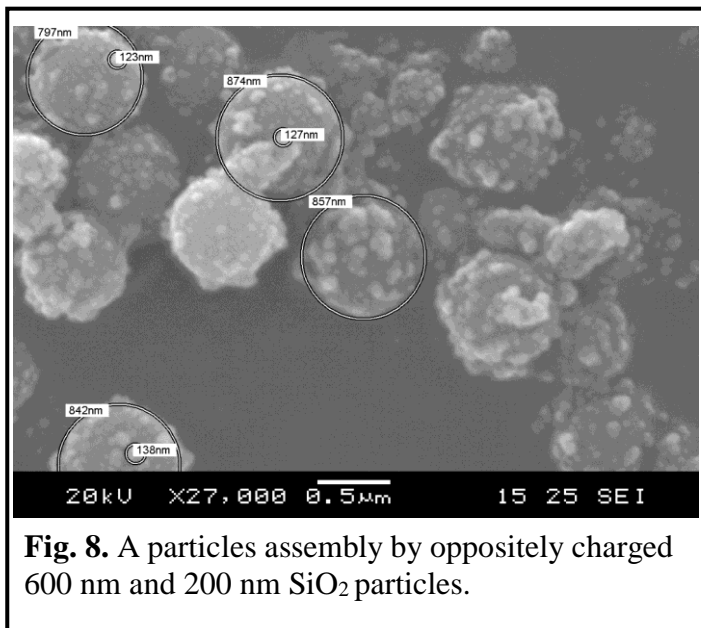
Fig. 8. A particles assembly by oppositely charged 600 nm and 200 nm SiO_2 particles.

8

solvation shell diameters of 849.1±6.2 nm on average, and -35.5±0.3 mV charges on the

surface (Table 2a). With positively charged $-N^+(CH_2CH_3)_2$ groups, 200 nm SiO_2 particles

showed solvation shell diameters of 911.0±18.6 nm on average and +21.6±0.9 mV

charges on the surface (Table 2b).

Table 2. Results of Zeta potential examinations of SiO_2 particles.

Size of SiO_2 particles		Functional group	Solvation shell diameter[a]	Charge[a]
a	600 nm	$-SO_3^-$	849.1±6.2 nm	-35.5±0.3 mV
b	200 nm	$-N^+(CH_2CH_3)_2$	911.0±18.6 nm	+21.6±0.9 mV

[a] the average number and deviation data is calculated based on three measurements, respectively.

The two potential numbers were both over 20 mV in their absolute values, which meant

that SiO_2 particles were charged stably. However, both of the size measurements were

bigger with 2SP nano-sizer machine, compared to SEM results, due to solvation effects.

Above values were calculated based on three measurements of each sample, respectively.

After assuring that the two particles were successively functionalized with

sufficient charges, two particle suspensions were mixed. Observable precipitation was

observed at the bottom of the vial after 1 hours of standing. The observable precipitation

indicates particle assembly, which was confirmed by SEM images shown in Fig 8. SEM

images shown that small negatively charged particles were attached to bigger positively

charged particles.

1.3. Experimental Details

1.3.1. Synthesis of Flower-structured PS-Cl

The solvent of the reaction comprised of 9.08 mL isopropanol and 1.329 mL toluene. Two precursors, Solution A and Solution B, were made before the synthesis.

Solution A was made with following procedures. Molecular wright of 360,000 g/mol PVP (0.195 g, 5.4×10^{-7} mol) was dissolved in 9.387 mL solvent aided by sonication in a 25 mL round bottom flask. 1.1536 mL styrene monomer de-prohibited by Aluminum oxide, Divinylbenzen (DVB, 24 µL, 2.0×10^{-4} mol) and 4-vinylbenzyl chloride (33.6 µL, 2.0×10^{-4} mol) were added into the reaction flask successively. The mixture was heated to 70ºC (120 rpm) under N_2 for 20 min to reach equilibrium.

Solution B was made by adding Azobisisobutyronitrile (AIBN, 0.078g, 4.8×10^{-4} mol) and styrene monomer (0.494 mL, 5.2×10^{-3} mol) de-prohibited by Aluminum oxide to 1 mL solvent successively.

Solution B was added into Solution A dropwise and the mixture was kept at equilibrium condition of Solution A for 24 hours. The resulting solution was centrifuged and the solid layer was washed with 10 mL methanol twice. Flower-structured PS-Cl particles were obtained and the SEM image is shown in Fig 4a.

1.3.2. Synthesis of Spherical PS-Cl

Isopropanol as the solvent was used. Two precursors, Solution A and Solution B, were made before the synthesis.

Solution A was made with following procedures. Molecular weight of 360,000 g/mol PVP (0.195 g, 5.4×10^{-7} mol) was dissolved in 10.032 mL solvent aided by sonication in a 25 mL round bottom flask. styrene monomer (1.1536 mL, 1.2×10^{-2} mol) de-prohibited by Aluminum oxide, DVB (0.164 mL, 1.4×10^{-3} mol) and 4-vinylbenzyl chloride (33.6 µL, 2.0×10^{-4} mol) were added into the reaction flask successively. The mixture was heated to 70°C and stirred (120 rpm) under N_2 for 20 min to reach equilibrium.

Solution B was made with following procedures. AIBN (0.052g, 3.2×10^{-4} mol) and styrene monomer (0.494 mL, 5.2×10^{-3} mol) de-prohibited by Aluminum oxide were added to 0.528 mL solvent successively.

Solution B was added into Solution A dropwise and the mixture was kept at equilibrium condition of Solution A for 24 hours. The resulting solution was centrifuged and the solid layer was washed with 10 mL methanol twice. Spherical PS-Cl particles were obtained and the SEM image is shown in Fig 4b. This sample was sent to Robertson Microlit Laboratory to get elementary analysis. The elementary analysis result is shown in Table 1a.

1.3.3. Synthesis of Positively Charged PS-Cl

10 mg of premade flower-structured PS-Cl particles and quinuodidine (56 mg, 5.0×10^{-4} mol) were added into N-methaylpyrrolidinone (NMP, 10 mL, 9.8×10^{-2} mol)

11

successively. The mixture was kept at room temperature (500 rpm) for 16 hours. The resulting mixture was centrifuged and the solid product was washed with ethanol, *N,N-*Dimethylformamide (DMF), tetrahydrofuran (THF), and ethanol twice each successively. The solid was then then dried at room temperature overnight. White solid positively charged PS-Cl particles were obtained. The reaction scheme is shown in Fig 5.

1.3.4. Synthesis of Negatively Charged PS-Cl

100 mg of premade spherical PS-Cl particles from were added to a mixture of 10 mL DMF, sodium 4-[(E)-(4-hydroxyphenyl)diazenyl]benzenesulfonate (40 mL, 8.9×10^{-2} mol) and 0.04 mL of 2.7 M sodium ethoxide in ethanol. The mixture was heated to 100 °C (500 rpm) for 16 hours. The resulting solution was centrifuged and the solid was washed with H_2O, DMF and ethanol successively and then air dried at room temperature overnight. White solid negatively charged PS-Cl particles were obtained. This sample was sent to Robertson Microlit Laboratory to get elementary analysis. The elementary analysis result is shown in Table 2b. The reaction scheme is shown in Fig 5.

1.3.5. Examination of Charged Particles Assemblies

3 mg of a negatively charged sample was dispensed in 0.4 mL DI water in a vial. 0.1 mL of upper layer clear suspensions was taken out and diluted with 1.4 mL water. The same procedures were carried out for a positively charged sample. 1.5 mL suspensions of two charged PS-Cl samples were made. The two suspensions were mixed and kept standing for 24 hours. No precipitation or aggregation was observed, which led us to look for other alternative materials.

1.3.6. Synthesis of SiO_2 Particles

18 mL DI water was added to 100 mL of ethanol in a round bottom flask. The mixture was equilibrated for 30 min (800 rpm) at room temperature for 600 nm particle and 45° C for 200 nm particle. After equilibration, 5 mL 29% NH_4OH and TEOS (7.5 mL, 3.9×10^{-2} mol) were added to the solution successively. The resulting solutions were stirred continually for 2.5 hours at their respective equilibration conditions. The resulting solutions were centrifuged and the solid products were washed twice with ethanol and dried at room temperature overnight. Spherical 600 nm and 200 nm SiO_2 particles were obtained. SEM images are shown in Fig 6.

1.3.7. Synthesis of Negatively Charged SiO2 Particles

0.0396g of 600 nm SiO_2 particles was placed into a 10 mL round bottom flask. 1 mL Toluene and (3-Mercaptopropyl)trimethoxysilane (MPTMS, 60 uL, 2.9×10^{-4} mol) were added into the flask successively at room temperature continuously stirring (300 RPM) for 24 hours. The resulting solution was centrifuged to afford the solid intermediate product. The intermediate product was washed twice with 1 mL ethanol twice and the solid product was dried at room temperature for 24 hours. 0.06g of the dried intermediate product was added to 1mL H_2O_2 at room temperature (340 rpm) under N_2 gas and stirred for 2 hours. The resulting solution was centrifuged to afford a second generation of solid intermediate. 51% H_2SO_4 (0.2 mL, 7.4×10^{-4} mol) and 1 mL H_2O was added into the second solid intermediate successively. The resulting solution was centrifuged and the solid was dried at room temperature overnight. Reaction Scheme is

13

shown in Fig 7. The potential of negatively charged 600 nm SiO_2 particles were measured with 2SP nano-sizer machine and the result is shown in Table 2a.

1.3.8. Synthesis of Positively Charged SiO_2 Particles

Positively charged $-N^+(CH_2CH_3)_3$ groups were added on to SiO_2 particles with following procedures. [19] 0.1g of 200 nm SiO_2 particles was added to 5 mL toluene in a 10 mL round bottom flask. (3-Aminopropyl)triethoxysilane (APTES, 0.186 mL, 8.9×10^{-4} mol) was added to the mixture at $120°C$ (760 rpm) for 24 hours. The resulting solution was centrifuged and the solid intermediate was washed with 1 mL ethanol twice and dried at room temperature overnight. 0.04g of the solid intermediate and CH_3CH_2I (0.3mL, 1.0×10^{-3} mol) was added successively into the mixture of 0.6g potassium carbonate and 5mL acetonitrile in a 10 mL round bottom flask. The mixture was heated to $62°C$ (460 rpm) for 45 hours. The resulting solution was centrifuged and the solid was washed with 1 mL of ethanol twice. Reaction Scheme is shown in Fig 7. The potential of positively charged 200 nm SiO_2 particles were measured with 2SP nano-sizer machine and the result is shown in Table 2b.

1.3.9. Dialysis and Assembly of Oppositely Charged Particles

SiO_2 particles with different charges were suspended in water and put into separate dialysis membranes. Membranes containing particle suspension were placed into Milli-Q water (500 rpm) at room temperature for 24 hours for dialysis. Particle dispersions were centrifuged and the solid products were collected and air dried at room

temperature overnight. 10^8 particles/ mL concentration solutions of both samples were made for the assembly. 1 mL of each solution was mixed and left sitting for 24 hours. A precipitation layer was observed on the bottom of the reaction vial. One drop of the suspension was put on carbon tape and dried over night to get ready for SEM. A SEM image of particle assembly is shown in Fig 8.

1.4. Discussion

Charged particles approach each other based on electrostatic attractions. Ideally, if charge and size are distributed evenly, negatively charged particles prefer to stay adjacent to positively charged particles, and vice versa (representation shows in Fig. 3a). The reason is that the charges normally can be neutralized when assembled with oppositely charged particles alternatively. However, the zeta potential measurements (Table. 2) by 2SP zeta sizer were averages of the detected particles. The particles that we functionalized don't have the exact same charge. We cannot exclude the possibility that some particles were functionalized more charged groups than others. When one particle has charges much higher than oppositely charged particles the system needs longer time to thermodynamically reach the lowest energy state. In Fig. 8, the majority of positively charged 200 nm particles are surrounding negatively charged 600 nm particles. However, some negatively charged 200 nm particles are observed on top of other negatively charged 200 nm particles. The reason could be due to the fact that some 600 nm particles were functionalized more positively charged than others, and therefore have higher

15

positive charges. The positive charges cannot be neutralized when they assemble together with negatively charged 200 nm particles, and therefore the whole particle cluster still has net positive charges to attract negatively charged 200 nm particles stacked on top of other 200 nm originally negatively charged particles. Therefore those 200 nm positively charged particles end up being adjacent to same charged particles (representation shows in Fig 3b). If given longer thermodynamic self-assembly time, some of the stacked 200 nm negatively charged particles might migrate to fulfill the vacancies on the positively charged 600 nm particles, until all the area is taken by 200 nm negatively charged particles.

1.5. The Future Work

Coworkers from theSchneebeli group will continue to work on this project to alter the size and charge of the oppositely charged particles, in order to obtain more complex and ordered structures. The highly ordered particle assembly products can (also be used as templates for) kinetic controlled led pattern replication.

1.6. References

(1)   Birol, H., Rambo, C. R., Guiotoku, M., & Hotza, D. (2013). Preparation of ceramic nanoparticles via cellulose-assisted glycine nitrate process: a review. *RSC Advances*, *3*(9), 2873-2884.
(2)   Sharafi, M. (2015). Toward Next Generation of Self-assembly. Unpublished manuscript.
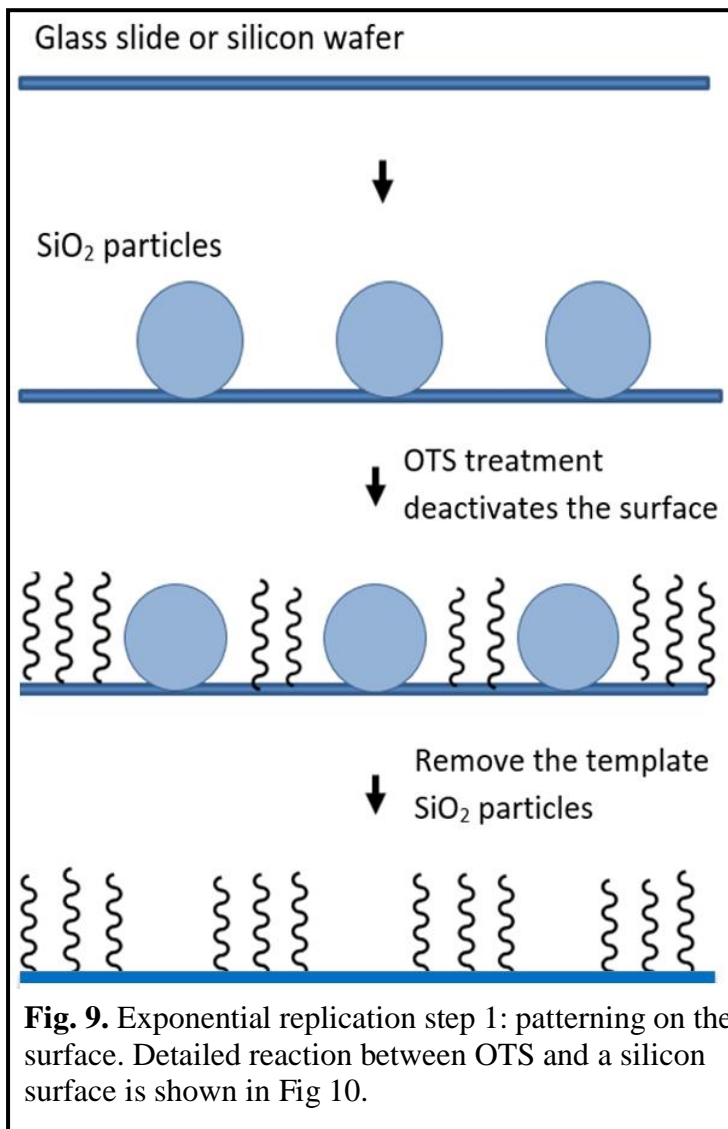(3)   Sharafi, M. (2015). Toward Colloidal Crystal with Long-Range Order. Unpublished manuscript.

(4)   Barisik, M., Atalay, S., Beskok, A., & Qian, S. (2014). Size dependent surface charge properties of silica nanoparticles. *The Journal of Physical Chemistry C*, *118*(4), 1836-1842.

(5)   Burns, A., Ow, H., & Wiesner, U. (2006). Fluorescent core–shell silica nanoparticles: towards "Lab on a Particle" architectures for nanobiotechnology. *Chemical Society Reviews*, *35*(11), 1028-1042.

(6)   Zhang, R., Jha, P. K., & de la Cruz, M. O. (2013). Non-equilibrium ionic assemblies of oppositely charged nanoparticles. *Soft Matter*, *9*(20), 5042-5051.

(7)   Kalsin, A. M., Kowalczyk, B., Smoukov, S. K., Klajn, R., & Grzybowski, B. A. (2006). Ionic-like behavior of oppositely charged nanoparticles. *Journal of the American Chemical Society*, *128*(47), 15046-15047.

(8)   Zhong, Y., Peng, F., Bao, F., Wang, S., Ji, X., Yang, L., & He, Y. (2013). Large-scale aqueous synthesis of fluorescent and biocompatible silicon nanoparticles and their use as highly photostable biological probes. *Journal of the American Chemical Society*, *135*(22), 8350-8356.

(9)   Zerrouki, D., Baudry, J., Pine, D., Chaikin, P., & Bibette, J. (2008). Chiral colloidal clusters. *Nature*, *455*(7211), 380-382.

(10)   Song, P., Wang, Y., Wang, Y., Hollingsworth, A. D., Weck, M., Pine, D. J., & Ward, M. D. (2015). Patchy Particle Packing under Electric Fields. *Journal of the American Chemical Society*, *137*(8), 3069-3075.

(11)   Yan, M., Fresnais, J., Sekar, S., Chapel, J. P., & Berret, J. F. (2011). Magnetic nanowires generated via the waterborne desalting transition pathway. *ACS applied materials & interfaces*, *3*(4), 1049-1054.

(12)   Pokroy, B., Kang, S. H., Mahadevan, L., & Aizenberg, J. (2009). Self-organization of a mesoscale bristle into ordered, hierarchical helical assemblies. *Science*, *323*(5911), 237-240.

(13)   Chen, Q., Bae, S. C., & Granick, S. (2011). Directed self-assembly of a colloidal kagome lattice. *Nature*, *469*(7330), 381-384.

(14)   Reese, C. E., Guerrero, C. D., Weissman, J. M., Lee, K., & Asher, S. A. (2000). Synthesis of highly charged, monodisperse polystyrene colloidal particles for the fabrication of photonic crystals. *Journal of colloid and interface science*, *232*(1), 76-80.

(15)   McCarty, L. S., Winkleman, A., & Whitesides, G. M. (2007). Electrostatic Self-Assembly of Polystyrene Microspheres by Using Chemically Directed Contact Electrification. *Angewandte Chemie International Edition*, *46*(1-2), 206-209.

(16)   Plumeré, N., Ruff, A., Speiser, B., Feldmann, V., & Mayer, H. A. (2012). Stöber silica particles as basis for redox modifications: Particle shape, size, polydispersity, and porosity. *Journal of colloid and interface science*, *368*(1), 208-219.

(17)   Nozawa, K., Gailhanou, H., Raison, L., Panizza, P., Ushiki, H., Sellier, E., ... & Delville, M. H. (2005). Smart control of monodisperse Stöber silica particles: effect of reactant addition rate on growth process. *Langmuir*, *21*(4), 1516-1523.

(18)   Farrukh, A., Akram, A., Ghaffar, A., Tuncel, E., Oluz, Z., Duran, H., & Yameen, B. (2014). Surface-functionalized silica gel adsorbents for efficient remediation of cationic dyes. *Pure and Applied Chemistry*, *86*(7), 1177-1188.

(19)   Cerneaux, S. A., Zakeeruddin, S. M., Grätzel, M., Cheng, Y. B., & Spiccia, L. (2008). New functional triethoxysilanes as iodide sources for dye-sensitized solar cells. *Journal of Photochemistry and Photobiology A: Chemistry*, *198*(2), 186-191.

2.1. Introduction

Pattern replication is common in both nature and industry. In nature, animals and plants replicate patterns from one generation to the next. In industry, stamping techniques, for example contact-printing[20] and nano-imprint lithography[21], are commonly used to replicate patterns. However, most man-made replication schemes are linear, which limits the efficiency of these processes.

This project focuses on realizing exponential replication of nanoscale patterns through kinetic control methods. The template pattern can either be made by photolithography, which required more complex instruments making this method inaccessible for our project, or can be made by thermodynamic particle assembly from Chapter 1,

Fig. 9. Exponential replication step 1: patterning on the surface. Detailed reaction between OTS and a silicon surface is shown in Fig 10.

19

or can be made by particle deposition, which is described in detail later in this chapter. This process uses an original pattern as a template to synthesize identical products. This process is exponential as the newly replicated products can be used as templates in the next replication cycles. Thus, just like DNA replication, 2^n products are formed after n replication cycles.

Prototypical, exponential flow diagrams are shown in Fig 9, 11 and 12. We start (Fig 9) with a glass slide or a silicon wafer, which is patterned by depositing SiO_2 particles. After binding the particles to the surface, a layer of octadecyltrichlorosilane (OTS) is added[22]. The OTS serves as a deactivation
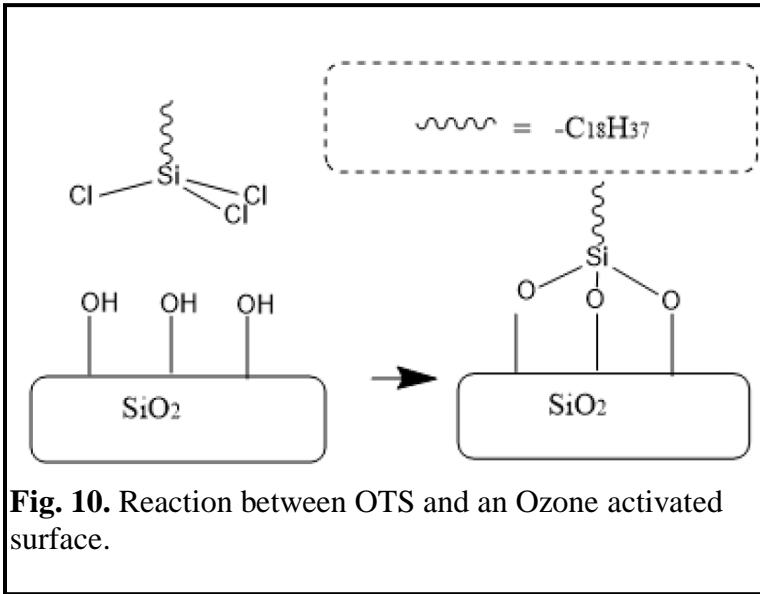
Fig. 10. Reaction between OTS and an Ozone activated surface.

layer to prevent growth of a "bridge layer" in these locations. Reaction between OTS and the silicon surface is shown in Fig 10. Next, SiO_2 particles are removed from the surface. Note that before OTS treatment, UV-ozone treatment is carried out to enhance the hydrophilicity[23] of the surface, increasing bonding strength between the surface and the silane functional groups of OTS, leaving the hydrophobic OTS chains pointing outwards. When the patterns are made on the surface, areas that were previously covered by SiO_2 particles will not change the hydrophilicity, which will direct the particle growth

kinetically. However, areas that were not previously covered by SiO_2 particles will be covered by OTS with hydrophobic tails pointing out, therefore those areas will be hydrophobic, and remain nonreactive in the later replication reactions. With these steps, which have already been carried out successfully (vide infra), patterning of the surface (Fig 9), is accomplished.

Fig. 11. Exponential replication step 2: first generations of replicas on the surface.
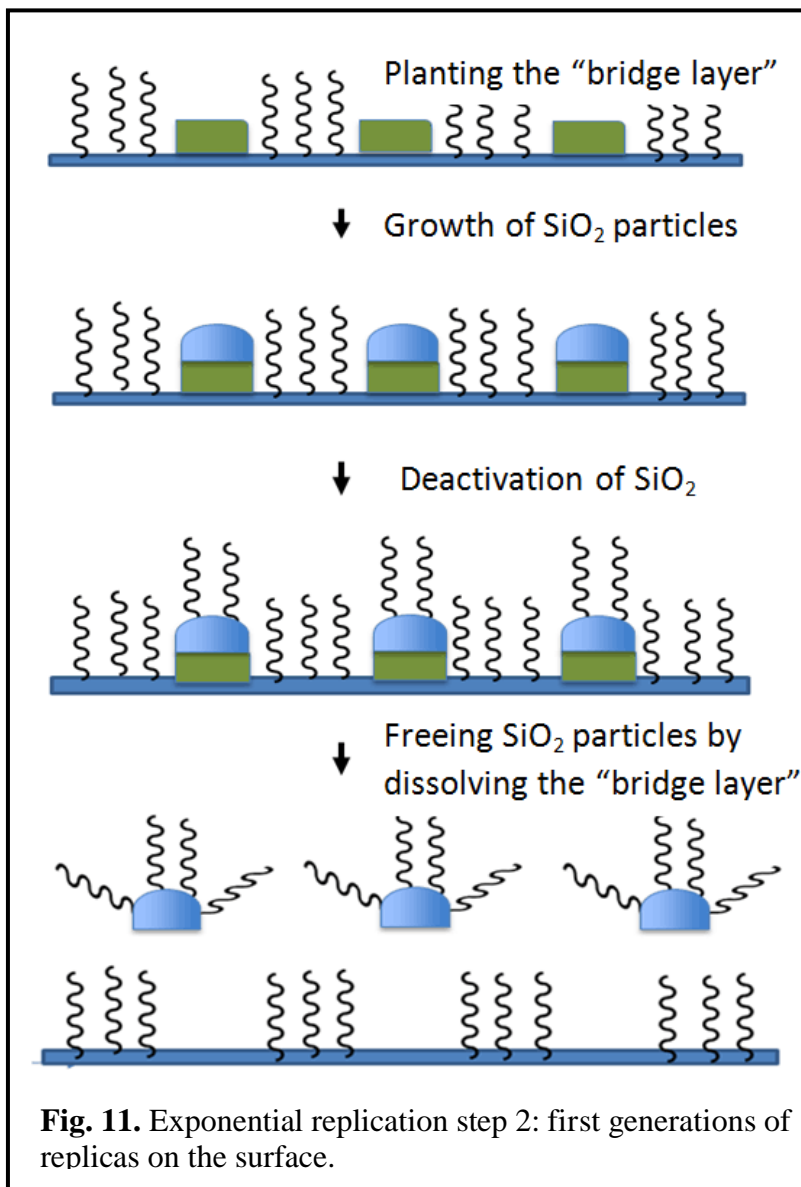
Step 2 involves replicating the first generation products on a surface (procedures are shown in Fig 11). A "bridge layer", is grown on the surface before the growth of the products in order to ensure the products can be separated from the surface after replication. An OTS layer is then grown again on top of the products to deactivate their outside surfaces. Then, the "bridge layer" is dissolved to free the products from the surface.

21

When we obtain products with OTS attached in solution, the second step (Fig 11) is finished. The products are now ready to go on to the solution phase of the exponential replication cycle.

Fig. 12 Exponential replication step 3: replication cycle.
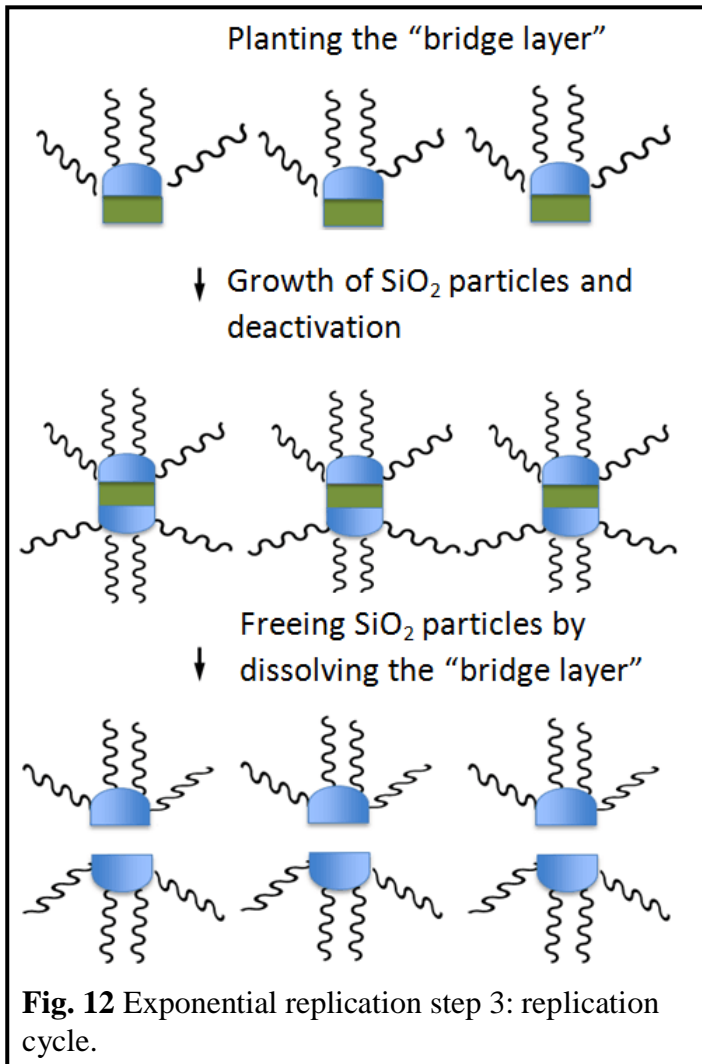
This third step, replication in solution, is shown in Fig 12. First, a "bridge layer" is formed again before the generation of the products and deactivation of the newly formed products by OTS treatment. Afterwards, the "bridge layer" is dissolved to separate the two generations of the products. Repeating this step n times, affords 2^n products. This process is exponential as compared to linear replication, which only leads to 2n products after n generations.

We anticipate that our exponential pattern replication method can not only improve the replication efficiency of common shapes, but can also be applied to more complex shapes, as long as the original foot print can be copied on the surface.

22

But why do we care about shapes?

On a molecular scale, materials with well-controlled shapes are widely used in chemical catalysis, molecular recognition, and artificial antibody targeting. For example, the electro-catalytic activity of 2,4,6-trinitrotoluene depends highly on the particle shape[24]. Another example is that shape control helps molecular recognition and biological targeting[25]. This is because matching shapes increases noncovalent interactions (H-bonding, π- π stacking and cation π interactions), between reactants and catalysts, drugs and receptors. In addition, on the nanoscale, properties could highly depend upon shapes. The relationship between a molecule's structure and its properties still needs to be studied further. Controlling a material's shape at the nanoscale remains a significant scientific challenge. In this project, templates are used to kinetically direct the formation of the chemical bonds. Once the shape of materials at the nanoscale can be controlled, more potential applications can be achieved.

In the project, we decided to produce SiO_2 as products, because these particles can be easily synthesized using the well-known Stöber's process.[26,27] SiO_2 particles are shown in Fig 4 in chapter 1. In addition, SiO_2 is a relatively environmentally friendly and nontoxic material. Conventional SiO_2 synthetic methods can hardly accomplish well-defined shapes. Conventional methods mostly use either physical routes, such as sputtering and physical vapor deposition, or chemical routes, such as chemical vapor deposition[28] and pyrolysis from precursor film[29]. These methods make it difficult to control the shape, and are typically carried out on small scales. However, with the pattern replication method shown in Fig 9, 11 and 12, products can be formed exponentially.

2.2. Results and Discussions

Uniform spherical 600 nm SiO_2 particles were synthesized via Stöber's process as
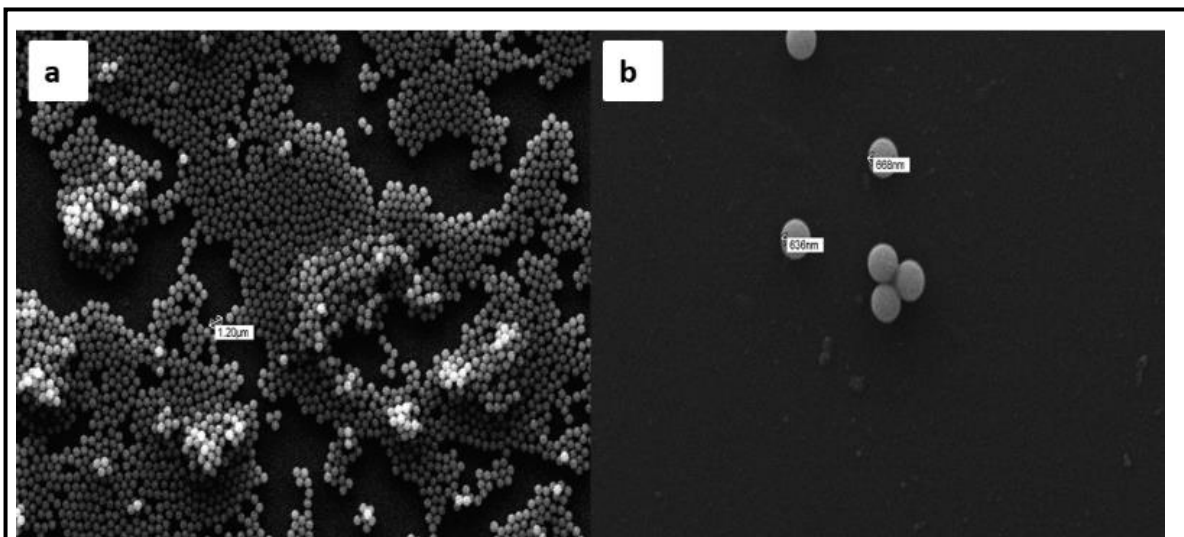
Fig. 13. SEM images of a Glass slide surface. a) Glass slide surface with SiO_2 particles before sonication. The particles were deposited on the surface by adding a SiO_2/EtOH solution drop-wise on a glass slides or silicon wafer, followed by 24 h of air-dried, UV-Ozone treatment and OTS treatment. b) SEM image of glass slide surface with SiO_2 particles after sonication.

described in chapter 1. The premade particles were used to create round patterns on silicon wafer and glass slides with OTS, following a process described by Bae and coworkers.[30] SEM images of the glass slide surface before and after sonication removal of the deposited SiO_2 are shown in Fig 13. Most of the template SiO_2 particles were removed. Patterns were made on the surface of the glass slide surface. The pattern imprints were
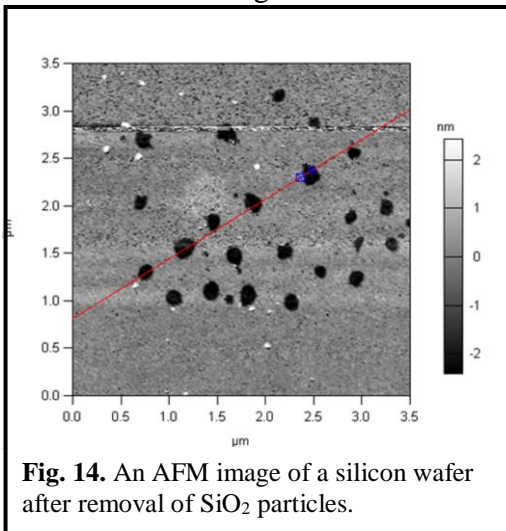
Fig. 14. An AFM image of a silicon wafer after removal of SiO_2 particles.

characterized by Atomic Force Microscopy (AFM), shown in Fig 14. The heights of the patterns averaged around 3-5 nm. The surface area can be up to 200 nm in diameter. The patterns appeared not completely uniform due to inconsistencies in size of the pattern particles, however considering the difficulties of making patterns at the nanoscale, it's relatively uniform for our purpose.
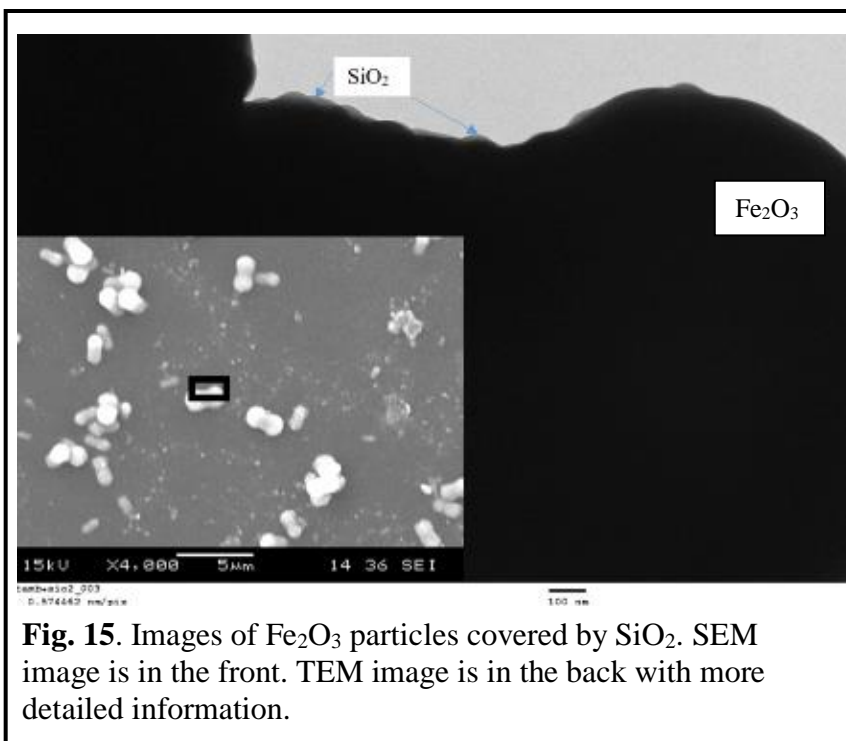
After assuring the pattern can be made on the surface, "bridge layer" material was explored. Finding the best fit "bridge layer" (Figs 9, 11, and 12.), which connects the template and product pieces, is the most challenging aspect of the replication process. During the tests to find a suitable bridge layer material, the pattern can be ignored -- it is only important at this point

Fig. 15. Images of Fe_2O_3 particles covered by SiO_2. SEM image is in the front. TEM image is in the back with more detailed information.

that the "bridge layer" and product pieces can grow are on one another. As a first attempt, Fe_2O_3 was chosen as the material for "bridge layer", because the reagents were readily available and nontoxic. Additionally, the synthesis was not air sensitive. Base on to previous experience and literature reviews, Fe_2O_3 can be easily grow on top of SiO_2 because of the wide capacity of the SiO_2 particles. However, growing Fe_2O_3 on SiO_2 has

25

proven to be a challenge in the past. In order to examine the growth of SiO_2 on top of Fe_2O_3, Fe_2O_3 particles were synthesized following a modified, previously reported procedure[31].Peanut shaped Fe_2O_3 particles and Cubic Fe_2O_3 particles were synthesized using an almost identical procedure, except Na_2SO_4 was not added for Cubic Particles.

SiO$_2$ layer was attempted to grow on Fe_2O_3 bridging material. To grow SiO_2 layer on top of the Fe_2O_3 Peanut shaped particles, revised Stöber's process described by Lu and coworkers was used.[32] Transmission Electron Microscopy (TEM) images showed that the SiO_2 only spotted on the Fe_2O_3 particles with a thickness of 5-15 nm with patches instead of growing the layer completely surrounding the Fe_2O_3 particles, which was
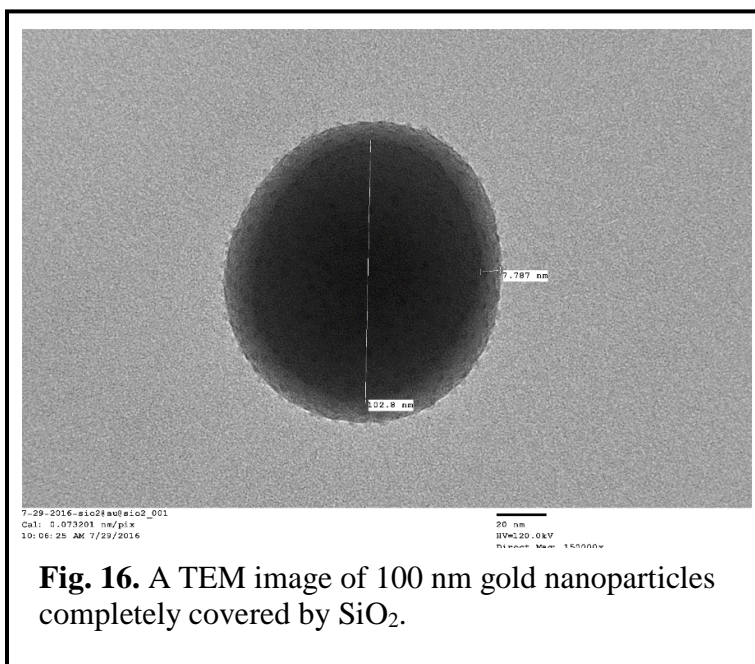
Fig. 16. A TEM image of 100 nm gold nanoparticles completely covered by SiO_2.

expected. In addition, 8 days of heating was required in the Fe_2O_3 particles synthesis process, which limited the progress of this project. Therefore, other materials, which could be easily synthesized and completely surrounded by a layer of SiO_2 particles were desired.

Au was chosen as a second generation "bridge layer" material. According to the procedures described by Van[33], gold particles can be grown readily on SiO_2 and SiO_2 can

26

also easily be grown on gold particles. The same examination was carried out to see if SiO_2 could grow on top of Au particles. 100 nm gold nanoparticles were made by following procedures previously reported in literature.[34] A SiO_2 layer was grown on top of the lab-made gold nanoparticles as described in literature procedures (SEM image in Fig 16) .[35]

Fig. 17. A TEM image of Au layer surrounding SiO_2 nanoparticles.
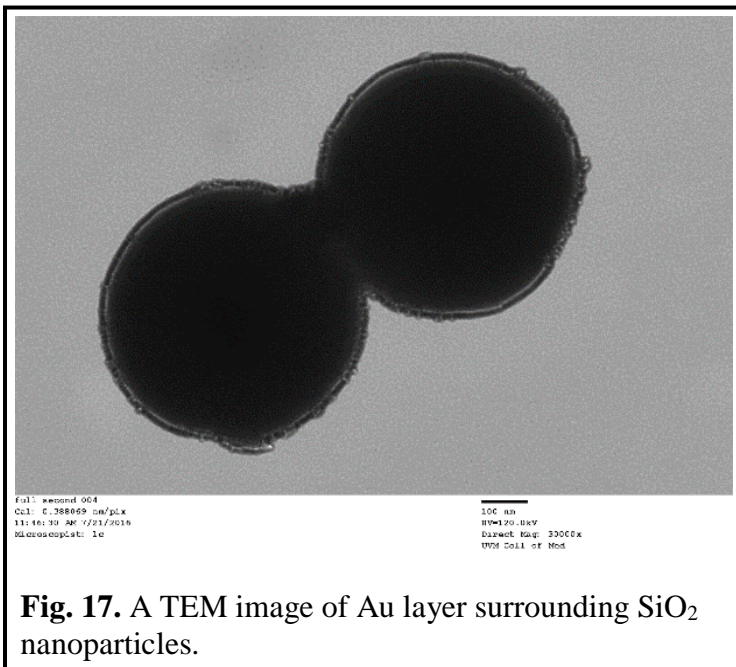
After confirming SiO_2 layer could be grown on top of gold nanoparticles, a gold "bridge layer" at this point was attempted to be grown on premade SiO_2 particles following a published procedure.[36] Waclawic and coworkers used 50 nm SiO_2 particle cores. In our experiment, 600 nm SiO_2 premade particle cores from chapter 1 were used because larger particles are easier to observe with microscopies. Procedures to grow a gold layer on premade 600 nm SiO_2 particles are similar to previously described method to synthesize gold nanoparticles (details will be shown in experiment session). TEM image of Au layer surrounding SiO_2 nanoparticles is shown in Fig 17.

Although the majority of SiO_2 particles were only spotted by Au colloidal, a small portion of SiO_2 particles were fully covered by Au layer was observed, which confirmed

27

the Au is promising to be a fit "bridge layer" material, if more experiments were carried out to obtain the best reaction conditions. On other hand, the not complete surrounding layer growth might have been caused by overly increase of SiO_2 particle surface area since we were using 600 nm particles instead of 50 nm described in the procedures described by English and coworkers. If smaller particles were used in the project, the percentage of the completely covered desired particles might well increase.

2.3. Experimental Details

2.3.1. Preparation of Patterned Surfaces

Approximately 0.1 g of SiO_2 is suspended in 1 mL of EtOH. The suspension was added onto the silicon surface dropwise and undergoes one hour of UV-Ozone treatment followed by five hours of OTS treatment. The template SiO_2 particles are then removed by sonication. SEM images of the surface before and after removal of the template particles are shown in Fig 13.

2.3.2. Synthesis of the Fe_2O_3 "Bridge Layer"

Peanut shaped Fe_2O_3 particles were synthesized by adding 5 mL of a 2.0 M $FeCl_3$ solution to a green cap vial. 4.5 mL of 6.0 M NaOH solution was added dropwise and the resulting mixture was stirred vigorously for 5 min. 0.5 mL of 0.60 M Na_2SO_4 solution was added and stirred continuously for another 10 min. The cap was closed tightly and the reaction vial was heated to 100 °C and stirred for 8 days. Afterward, the green vial was cooled to room temperature using a water bath. The reaction solution was decanted and the bottom layer was centrifuged. The resulting solid was washed with DI water 3

28

times before drying at room temperature for 48 hours. Cubic Fe_2O_3 particles (Fig X) were synthesized using an almost identical procedure, except Na_2SO_4 was not added.

2.3.3. Synthesis of SiO_2 on Fe_2O_3 Particles

A solution of 20 mL 100% ethanol, 1 mL DI water, and 5 mL 28% NH_4OH was prepared in a 50 mL round bottom flask. 0.12 g of peanuts shaped Fe_2O_3 was then added. The resulting suspension was sonicated at 50 °C for X hours. 0.25 mL of TEOS was added dropwise into the reaction flask. After the addition of TEOS, the reaction was sonicated for 5 hours. Afterward, the resulting mixture was centrifuged. The solid was collected and washed 3 times with DI water and 100% ethanol before drying at room temperature overnight. The SEM and TEM images of solid peanut shaped Fe_2O_3 Particles spotted by SiO_2 colloids are shown in Fig 15. Since SiO_2 didn't completely cover Fe_2O_3 Particles, second candidate needed to be explored.

2.3.4. Synthesis of the Gold "Bridge Layer"

1 mL 1% $HAuCl_4$ was added into 90 mL Milli-Q water in a 250 mL round bottom flask and stirred. 2 mL of 38.8 M sodium citrate was added to the reaction vessel. After stirring for 1 min, 1 mL of fresh $NaBH_4$ solution (13 mg $NaBH_4$ in 5 mL 38.8 M sodium citrate) was added dropwise forming a ruby-red solution. The mixture was stirred at 4 °C for 30 min and left at 4 °C for another 10 hours. The resulting solution was centrifuged and solid particles were washed with citrate acid (pH=6.4) 3 times and dissolved in 1mL of citrate acid. The solution was labeled as solution I and saved for later uses. 25 mg of K_2CO_3 was dissolved in 100 mL of Milli-Q water. After 10 min, 1.5 mL of a 1% $HAuCl_4$ was added to the K_2CO_3 solution. The $HAuCl_4/K_2CO_3$ solution (10 mL) was aged for 1

day and placed into a 50 mL flask. [37] The solution was stirred vigorously while 50 µl of 29% formaldehyde was added dropwise. Approximately 100 µl solution I was added into the mixture and stirred for 10 min. The resulting solution was centrifuged and the solid gold nanoparticles were washed with Milli-Q water twice and finally suspended in 1 mL Milli-Q water, affording 100 nm gold nanoparticle suspension.

2.3.5. Synthesis of SiO_2 Layer on Gold Nanoparticles

40 mL of the gold nanoparticle suspension was added to a mixture of 0.5 mL ammonia solution in 20 mL 2-proponal. 56 µl TEOS was added and stirred for 1 hour at room temperature. The resulting solution was centrifuged and decanted to afford the desired Au@SiO_2 complexes. The particles were washed with DI water twice. 8-10 nm SiO_2 layer was grown on top surrounding 100 nm gold nanoparticles completely as shown in Fig 16.

2.3.6. Synthesis of Gold Layer on SiO_2 Nanoparticles

10 mg premade 600 nm SiO_2 particles were suspended in 20 mL ethanol aided by sonication. 0.05 mL (3-Aminopropyl)triethoxysilane (APTES) was added and stirred at 120°C for 2 hours. The resulting solution was centrifuged and washed with ethanol 3 times to afford the amine functionalized SiO_2 particles. The solid particles were suspended in 10 mL ethanol. 5 mL of the suspension was added into the gold solution and left sitting for10 hours at 4°C. The resulting suspension was centrifuged and the solid was washed with ethanol twice. A TEM image of SiO_2 covered with Au layer is shown in Fig 17.

2.4. The Future Work

Coworkers from the Schneebeli's group will continue to work on optimizing the size of SiO_2 inner cores to afford more fully covered particles. After confirming the "bridge layer" material, templates can be used to achieve exponential replication. The template can either be made by particle deposition in Fig 9 or can be derived by thermodynamically assembled crystal surfaces. Further, if inorganic materials with well-defined shapes are successfully formed, this process can be expanded to more complex organic polymers with specific morphologies. This can be realized by controlled radical polymerizations, if the two generations of shapes are provided with an appropriate amount of organic bridging materials to connect to each other.

2.5. References

(20)   Fan, Z., Ho, J. C., Jacobson, Z. A., Yerushalmi, R., Alley, R. L., Razavi, H., & Javey, A. (2008). Wafer-scale assembly of highly ordered semiconductor nanowire arrays by contact printing. *Nano letters*, *8*(1), 20-25.
(21)   Han, K. S., Shin, J. H., Yoon, W. Y., & Lee, H. (2011). Enhanced performance of solar cells with anti-reflection layer fabricated by nano-imprint lithography. *Solar Energy Materials and Solar Cells*, *95*(1), 288-291.
(22)   Miozzo, L., Yassar, A., & Horowitz, G. (2010). Surface engineering for high performance organic electronic devices: the chemical approach. *Journal of Materials Chemistry*, *20*(13), 2513-2538.
(23)   Oláh, A., Hillborg, H., & Vancso, G. J. (2005). Hydrophobic recovery of UV/ozone treated poly (dimethylsiloxane): adhesion studies by contact mechanics and mechanism of surface modification. *Applied Surface Science*, *239*(3), 410-423.
(24)   Soomro, R. A., Akyuz, O. P., Akin, H., Ozturk, R., & Ibupoto, Z. H. (2016). Highly sensitive shape dependent electro-catalysis of TNT molecules using Pd and Pd–Pt alloy based nanostructures. *RSC Advances*, *6*(51), 44955-44962.
(25)   Endo, T., Tajima, K., Yamashita, M., Ito, M. M., Nishida, J. I., & Ogikubo, T. (1986). Control of the degree of molecular recognition by shape-specific weak interactions between nonpolar groups. *Journal of the Chemical Society, Chemical Communications*, (21), 1561-1562.

(26)   Liz-Marzán, L. M., Giersig, M., & Mulvaney, P. (1996). Synthesis of nanosized gold-silica core-shell particles. *Langmuir*, *12*(18), 4329-4335.

(27)   Stöber, W., Fink, A., & Bohn, E. (1968). Controlled growth of monodisperse silica spheres in the micron size range. *Journal of colloid and interface science*, *26*(1), 62-69.

(28)   Okumura, M., Tsubota, S., & Haruta, M. (2004). Vital role of moisture in the catalytic activity of supported gold nanoparticles. *Angewandte Chemie International Edition*, *43*(16), 2129-2132.

(29)   Kinoshita, H., Murakami, T., & Fukushima, F. (2004). Chemical vapor deposition of SiO_2 films by $TEOS/O_2$ supermagnetron plasma. *Vacuum*, *76*(1), 19-22.

(30)   Bae, C., Moon, J., Shin, H., Kim, J., & Sung, M. M. (2007). Fabrication of monodisperse asymmetric colloidal clusters by using contact area lithography (CAL). *Journal of the American Chemical Society*, *129*(46), 14232-14239.

(31)   Li, M., Li, X., Qi, X., Luo, F., & He, G. (2015). Shape-Controlled Synthesis of Magnetic Iron Oxide@ SiO_2–Au@ C Particles with Core–Shell Nanostructures. *Langmuir*, *31*(18), 5190-5197.

(32)   Cai, Z., Leong, E. S., Wang, Z., Niu, W., Zhang, W., Ravaine, S., & Lu, X. (2015). Sandwich-structured Fe_2O_3@ SiO_2@ Au nanoparticles with magnetoplasmonic responses. *Journal of Materials Chemistry C*, *3*(44), 11645-11652.

(33)   Graf, C., & van Blaaderen, A. (2002). Metallodielectric colloidal core-shell particles for photonic applications. *Langmuir*, *18*(2), 524-534.

(34)   Qu, Y., Porter, R., Shan, F., Carter, J. D., & Guo, T. (2006). Synthesis of tubular gold and silver nanoshells using silica nanowire core templates. *Langmuir*, *22*(14), 6367-6374.

(35)   Lu, Y., Yin, Y., Li, Z. Y., & Xia, Y. (2002). Synthesis and self-assembly of Au@ SiO_2 core-shell colloids. *Nano Letters*, *2*(7), 785-788.

(36) English, M. D., & Waclawik, E. R. (2012). A novel method for the synthesis of monodisperse gold-coated silica nanoparticles. *Journal of Nanoparticle Research*, *14*(1), 1-10.

(37) Pham, T., Jackson, J. B., Halas, N. J., & Lee, T. R. (2002). Preparation and characterization of gold nanoshells coated with self-assembled monolayers. *Langmuir*, *18*(12), 4915-4920.

COMPREHENSIVE REFERENCE

Bae, C., Moon, J., Shin, H., Kim, J., & Sung, M. M. (2007). Fabrication of monodisperse asymmetric colloidal clusters by using contact area lithography (CAL). *Journal of the American Chemical Society*, *129*(46), 14232-14239.

Barisik, M., Atalay, S., Beskok, A., & Qian, S. (2014). Size dependent surface charge properties of silica nanoparticles. *The Journal of Physical Chemistry C*, *118*(4), 1836-1842.

Birol, H., Rambo, C. R., Guiotoku, M., & Hotza, D. (2013). Preparation of ceramic nanoparticles via cellulose-assisted glycine nitrate process: a review. *RSC Advances*, *3*(9), 2873-2884.

Burns, A., Ow, H., & Wiesner, U. (2006). Fluorescent core–shell silica nanoparticles: towards "Lab on a Particle" architectures for nanobiotechnology. *Chemical Society Reviews*, *35*(11), 1028-1042.

Cai, Z., Leong, E. S., Wang, Z., Niu, W., Zhang, W., Ravaine, S., & Lu, X. (2015). Sandwich-structured Fe_2O_3@ SiO_2@ Au nanoparticles with magnetoplasmonic responses. *Journal of Materials Chemistry C*, *3*(44), 11645-11652.

Cerneaux, S. A., Zakeeruddin, S. M., Grätzel, M., Cheng, Y. B., & Spiccia, L. (2008). New functional triethoxysilanes as iodide sources for dye-sensitized solar cells. *Journal of Photochemistry and Photobiology A: Chemistry*, *198*(2), 186-191.

Chen, Q., Bae, S. C., & Granick, S. (2011). Directed self-assembly of a colloidal kagome lattice. *Nature*, *469*(7330), 381-384.

Endo, T., Tajima, K., Yamashita, M., Ito, M. M., Nishida, J. I., & Ogikubo, T. (1986). Control of the degree of molecular recognition by shape-specific weak interactions between nonpolar groups. *Journal of the Chemical Society, Chemical Communications*, (21), 1561-1562.

English, M. D., & Waclawik, E. R. (2012). A novel method for the synthesis of monodisperse gold-coated silica nanoparticles. *Journal of Nanoparticle Research*, *14*(1), 1-10.

Fan, Z., Ho, J. C., Jacobson, Z. A., Yerushalmi, R., Alley, R. L., Razavi, H., & Javey, A. (2008). Wafer-scale assembly of highly ordered semiconductor nanowire arrays by contact printing. *Nano letters*, *8*(1), 20-25.

Farrukh, A., Akram, A., Ghaffar, A., Tuncel, E., Oluz, Z., Duran, H., & Yameen, B. (2014). Surface-functionalized silica gel adsorbents for efficient remediation of cationic dyes. *Pure and Applied Chemistry*, *86*(7), 1177-1188.

Graf, C., & van Blaaderen, A. (2002). Metallodielectric colloidal core-shell particles for photonic applications. *Langmuir*, *18*(2), 524-534.

Han, K. S., Shin, J. H., Yoon, W. Y., & Lee, H. (2011). Enhanced performance of solar cells with anti-reflection layer fabricated by nano-imprint lithography. *Solar Energy Materials and Solar Cells*, *95*(1), 288-291.

Kalsin, A. M., Kowalczyk, B., Smoukov, S. K., Klajn, R., & Grzybowski, B. A. (2006). Ionic-like behavior of oppositely charged nanoparticles. *Journal of the American Chemical Society*, *128*(47), 15046-15047.

Kinoshita, H., Murakami, T., & Fukushima, F. (2004). Chemical vapor deposition of SiO_2 films by $TEOS/O_2$ supermagnetron plasma. *Vacuum*, *76*(1), 19-22.

Li, M., Li, X., Qi, X., Luo, F., & He, G. (2015). Shape-Controlled Synthesis of Magnetic Iron Oxide@ SiO_2–Au@ C Particles with Core–Shell Nanostructures. *Langmuir*, *31*(18), 5190-5197.

Liz-Marzán, L. M., Giersig, M., & Mulvaney, P. (1996). Synthesis of nanosized gold-silica core-shell particles. *Langmuir*, *12*(18), 4329-4335.

Lu, Y., Yin, Y., Li, Z. Y., & Xia, Y. (2002). Synthesis and self-assembly of Au@ SiO_2 core-shell colloids. *Nano Letters*, *2*(7), 785-788.

McCarty, L. S., Winkleman, A., & Whitesides, G. M. (2007). Electrostatic Self-Assembly of Polystyrene Microspheres by Using Chemically Directed Contact Electrification. *Angewandte Chemie International Edition*, *46*(1-2), 206-209.

Miozzo, L., Yassar, A., & Horowitz, G. (2010). Surface engineering for high performance organic electronic devices: the chemical approach. *Journal of Materials Chemistry*, *20*(13), 2513-2538.

Nozawa, K., Gailhanou, H., Raison, L., Panizza, P., Ushiki, H., Sellier, E., ... & Delville, M. H. (2005). Smart control of monodisperse Stöber silica particles: effect of reactant addition rate on growth process. *Langmuir*, *21*(4), 1516-1523.

Okumura, M., Tsubota, S., & Haruta, M. (2004). Vital role of moisture in the catalytic activity of supported gold nanoparticles. *Angewandte Chemie International Edition*, *43*(16), 2129-2132.

Oláh, A., Hillborg, H., & Vancso, G. J. (2005). Hydrophobic recovery of UV/ozone treated poly (dimethylsiloxane): adhesion studies by contact mechanics and mechanism of surface modification. *Applied Surface Science*, *239*(3), 410-423.

Pham, T., Jackson, J. B., Halas, N. J., & Lee, T. R. (2002). Preparation and characterization of gold nanoshells coated with self-assembled monolayers. *Langmuir*, *18*(12), 4915-4920.

Plumeré, N., Ruff, A., Speiser, B., Feldmann, V., & Mayer, H. A. (2012). Stöber silica particles as basis for redox modifications: Particle shape, size, polydispersity, and porosity. *Journal of colloid and interface science*, *368*(1), 208-219.

Pokroy, B., Kang, S. H., Mahadevan, L., & Aizenberg, J. (2009). Self-organization of a mesoscale bristle into ordered, hierarchical helical assemblies. *Science*, *323*(5911), 237-240.

Qu, Y., Porter, R., Shan, F., Carter, J. D., & Guo, T. (2006). Synthesis of tubular gold and silver nanoshells using silica nanowire core templates. *Langmuir*, *22*(14), 6367-6374.

Reese, C. E., Guerrero, C. D., Weissman, J. M., Lee, K., & Asher, S. A. (2000). Synthesis of highly charged, monodisperse polystyrene colloidal particles for the fabrication of photonic crystals. *Journal of colloid and interface science*, *232*(1), 76-80.

Sharafi, M. (2015). Toward Next Generation of Self-assembly. Unpublished manuscript.

Sharafi, M. (2015). Toward Colloidal Crystal with Long-Range Order. Unpublished manuscript.

Song, P., Wang, Y., Wang, Y., Hollingsworth, A. D., Weck, M., Pine, D. J., & Ward, M. D. (2015). Patchy Particle Packing under Electric Fields. *Journal of the American Chemical Society*, *137*(8), 3069-3075.

Soomro, R. A., Akyuz, O. P., Akin, H., Ozturk, R., & Ibupoto, Z. H. (2016). Highly sensitive shape dependent electro-catalysis of TNT molecules using Pd and Pd–Pt alloy based nanostructures. *RSC Advances*, *6*(51), 44955-44962.

Stöber, W., Fink, A., & Bohn, E. (1968). Controlled growth of monodisperse silica spheres in the micron size range. *Journal of colloid and interface science*, *26*(1), 62-69.

Yan, M., Fresnais, J., Sekar, S., Chapel, J. P., & Berret, J. F. (2011). Magnetic nanowires generated via the waterborne desalting transition pathway. *ACS applied materials & interfaces*, *3*(4), 1049-1054.

Zerrouki, D., Baudry, J., Pine, D., Chaikin, P., & Bibette, J. (2008). Chiral colloidal clusters. *Nature*, *455*(7211), 380-382.

Zhang, R., Jha, P. K., & de la Cruz, M. O. (2013). Non-equilibrium ionic assemblies of oppositely charged nanoparticles. *Soft Matter*, *9*(20), 5042-5051.

Zhong, Y., Peng, F., Bao, F., Wang, S., Ji, X., Yang, L., & He, Y. (2013). Large-scale aqueous synthesis of fluorescent and biocompatible silicon nanoparticles and their use as highly photostable biological probes. *Journal of the American Chemical Society*, *135*(22), 8350-8356.